

# FABRICATIONS OF SUPER-HYDROPHOBIC SURFACES ON GLASS SLIDES AND THEIR ANTIICING BEHAVIOR

L. YU<sup>1\*</sup>, Q. S. PU<sup>2</sup>, J. YUAN<sup>3</sup>, X. D. ZHANG<sup>1</sup>, J. X. GAO<sup>1</sup>, S. M. LIU<sup>1</sup>

<sup>1</sup> College of Mechanics and Materials, Hohai University, Nanjing, P. R. China

<sup>2</sup> Xuzhou Supervision Center of Water Conservancy Constructions, Xuzhou, P. R. China

<sup>3</sup> Changjiang River Scientific Research Institute, Wuhan, P. R. China

*Superhydrophobic Co<sub>3</sub>O<sub>4</sub> surfaces with a micro-nanostructure on glass slides were successfully prepared using a simple solvothermal synthesis process at 160°C and dip-coatings with stearic acids to reduce the surface energy. Such surfaces showed superhydrophobic with a contact angle as high as approximately 169° and a low sliding angle of less than 3°. Further investigations indicated that the surfaces exhibited extraordinary self-cleaning performance and stable anti-icing property. For a spherical water droplet placed on the surfaces at -5°C, icing cannot occur for more than 70 min, implying wide applications on various industrial aspects.*

**Keywords:** Superhydrophobic; antiicing; contact angle

## 1. Introduction

Ice disaster is a serious problem in Iceland, Canada, Russia, Finland, Norway, USA, and even in China and Japan [1-5]. Each year, it seriously threatens on people's daily life, industrial and agricultural production because icing leads to material damage to outdoor equipment, including power transmission and distribution, telecommunication networks, boats, aircraft, etc. [1,2]. In order to reduce the ice disaster, various anti-icing methods have been developed, such as thermal deicing method, mechanical deicing method and so on. However, these traditional methods at the cost of high energy consumption cannot fundamentally solve the problem.

Inspired by the so called lotus effect [6,7], superhydrophobic surfaces (SHS) with a water contact angle (CA) greater than 150° and a very low sliding angle, typically below 10°, have attracted much interest from researchers because of their potential anti-icing properties [8-10]. In addition, such surfaces could be applied in daily life, agriculture and many industrial processes, such as antiadhesive coatings, self-cleaning materials, antifouling, anticorrosion, reduction of drag for micro-fluid and so forth [11-13]. Over the past decades, many exploratory researches have prepared artificial superhydrophobic surfaces through two different processes: one is fabricating a micro-nanostructures rough surface on low surface energy materials using fluorocarbons, silicones, other organic and inorganic materials such as ZnO and TiO<sub>2</sub>. Another alternative is creating a micro-

nanostructures rough surface first and then chemically modifying the surface with low surface energy materials. Based on the above processes, various methods for fabricating superhydrophobic surfaces have been reported: chemical vapor deposition, etching processing, electrochemistry method, sol-gel, layer-by-layer assembling method, etc. However, many of the methods involve multistep procedures and difficult process controls, or need specialized reagents and equipment.

In this work, we present a simple way to prepare superhydrophobic Co<sub>3</sub>O<sub>4</sub> films with micro-nanostructure via a solvothermal procedure. Here it should be pointed out that Co<sub>3</sub>O<sub>4</sub> thin films are already used in the industry as functional layers. For such functional materials, it is therefore important to seek their potential, especially, practical applications. To this end, we used the prepared superhydrophobic Co<sub>3</sub>O<sub>4</sub> films to achieve excellent anti-icing properties.

## 2. Experimental

In a typical experiment procedure, 1.0 g Co(NO<sub>3</sub>)<sub>2</sub>·6H<sub>2</sub>O and 0.01g cetyltrimethylammonium bromide (CTAB) were added to 10 mL absolute ethanol under magnetic stirring vigorously for 10min to form a homogeneous solution, which was then transferred into a Teflon-lined stainless steel autoclave. A glass slide (2×3 cm<sup>2</sup>) substrate was vertically placed in the reaction solution after ultrasonically cleaned in acetone, absolute ethanol and distilled water for 10 min each using an ultrasonic cleaner with a frequency of 50 kHz. The autoclave was sealed tightly and maintained at

\* Author corespondent/Corresponding author,  
E-mail: hyqgxu@126.com.

160°C for 90 min. After the solvothermal procedure, the autoclave cooled naturally down to the room temperature. The as-prepared Co<sub>3</sub>O<sub>4</sub> micro-nanostructure films were removed from the solution, and rinsed with absolute ethanol and then dried at 80°C for 2h. To achieve surface superhydrophobicity, the films were immersed in 1 wt.% absolute ethanol solution of stearic acids for 30 min at room temperature and then dried at 80°C.

The operation concerning icing experiments is described as follows. Smooth surface, hydrophobic surface and superhydrophobic surface, which corresponded to three different glass slides and were characterized subsequently, were placed into a fridge where the temperature were controlled at -5 °C using the infrared thermometer. The 9μl tap water drops with room temperature were placed on the above mentioned different surfaces, respectively. Before the experiment, the drops were liquid and transparent on the surfaces, and then they had apparent change in appearance because of icing. Occurrence of icing was observed by eye inspection. The anti-icing behavior of the SHSs was determined by the delay times during which the drop changed from the colorless transparent liquid to the white opaque solid. Or in other words, the measured period of time reflected the freezing process. After the first water drop freezed on the smooth surface, the delay times began to be recorded using a camera (Qingtao, Shanghai) every five minutes until all the droplets were frozen. The experiment was repeated 3 times in the same condition, values of the delay times were an average.

The phase purity of the products was examined by X-ray powder diffraction (XRD) using a Rigaku D/max 2500 diffractometer with Cu Kα radiation ( $k = 1.5406 \text{ \AA}$ ). Scanning electron microscopy (SEM) images were obtained using a JOEL JSM-6610LV microscope (Japan). Static contact angles and sliding angles were measured based on the sessile drop measuring method with 5μl droplets of distilled water using a Model 250 (p/n 250-F1) goniometer (ramé-hart instrument Co., USA) at ambient temperature. Average CAs were obtained by measuring the same sample at five different positions.

### 3. Results and discussion

Fig. 1 shows the X-ray diffraction (XRD) patterns of Co<sub>3</sub>O<sub>4</sub> films for different reaction time. As seen, all the diffraction peaks were attributed to Co<sub>3</sub>O<sub>4</sub>, indicating that the prepared films were single phase. Fig. 1(b and c) shows XRD patterns of Co<sub>3</sub>O<sub>4</sub> films prepared with and without CTAB for 90 min., respectively. The uniform XRD of the two films indicates that there is no effect of CTAB on the micro-nanostructure of the Co<sub>3</sub>O<sub>4</sub> films. However, both films are quite distinct from the

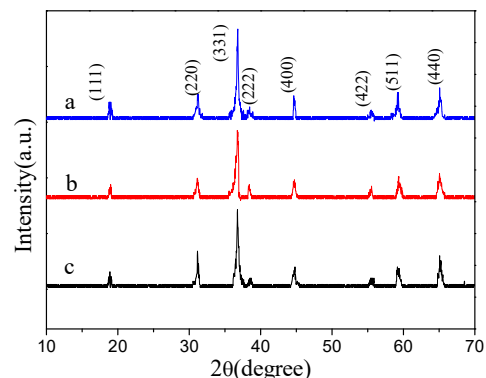
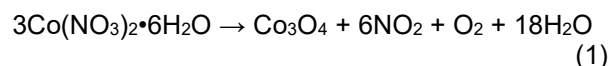


Fig. 1 - XRD patterns of the Co<sub>3</sub>O<sub>4</sub> film samples: (a) sample with adding CTAB for 60 min; (b) sample with adding CTAB for 90 min; (c) sample without adding CTAB for 90 min.

macroscopic (using visual observations). The former is uniform and compact, while the latter is rough, sparse and has obvious scallops (it looks like shells) in the interior of the film. The possible reason is that large amounts of gas are formed at the thermal treatment temperature, such as the volatile gaseous ethanol and the nitrogenous gas due to the decomposition of Co(NO<sub>3</sub>)<sub>2</sub>·6H<sub>2</sub>O to Co<sub>3</sub>O<sub>4</sub>, i.e.,



Here it is noted that multiple gasses can be generated during the decomposition, but no nitrogenous gas appears. Without CTAB in solution, these gases might stick to the glass slide with high surface tension in the form of bubbles and affect Co<sub>3</sub>O<sub>4</sub> crystal formation and growth on the surface. In the presence of CTAB, the surface tension is decreased resulting in complete wetting of the glass substrate and hence pore-free films are obtained [14].

Fig. 2 shows the SEM images of the prepared films. Fig. 2a shows the SEM images of Co<sub>3</sub>O<sub>4</sub> films after a 90 min of solvothermal synthesis time. It can be seen that morphology of the samples is made up of different size and uneven distributed sphere-like. The high magnification SEM image shown in Fig. 2b reveals that the sphere-like has no other structure growing on the surface. However, it is found that the sphere-like surface is rough due to embossments and grooves form the insets providing higher-magnification SEM images. The microphotographs in Fig. 2 (c and d) show the morphology of the as-prepared Co<sub>3</sub>O<sub>4</sub> films after a 90 min of reaction time at low magnification and at high magnification, respectively. From Fig. 2c, one can see that the sphere-like are dense and well-distributed at a large scale on the substrate. Fig. 2d reveals that many white nanometer particles are formed on the surface, and the secondary texture helps to construct micro-nanostructure.

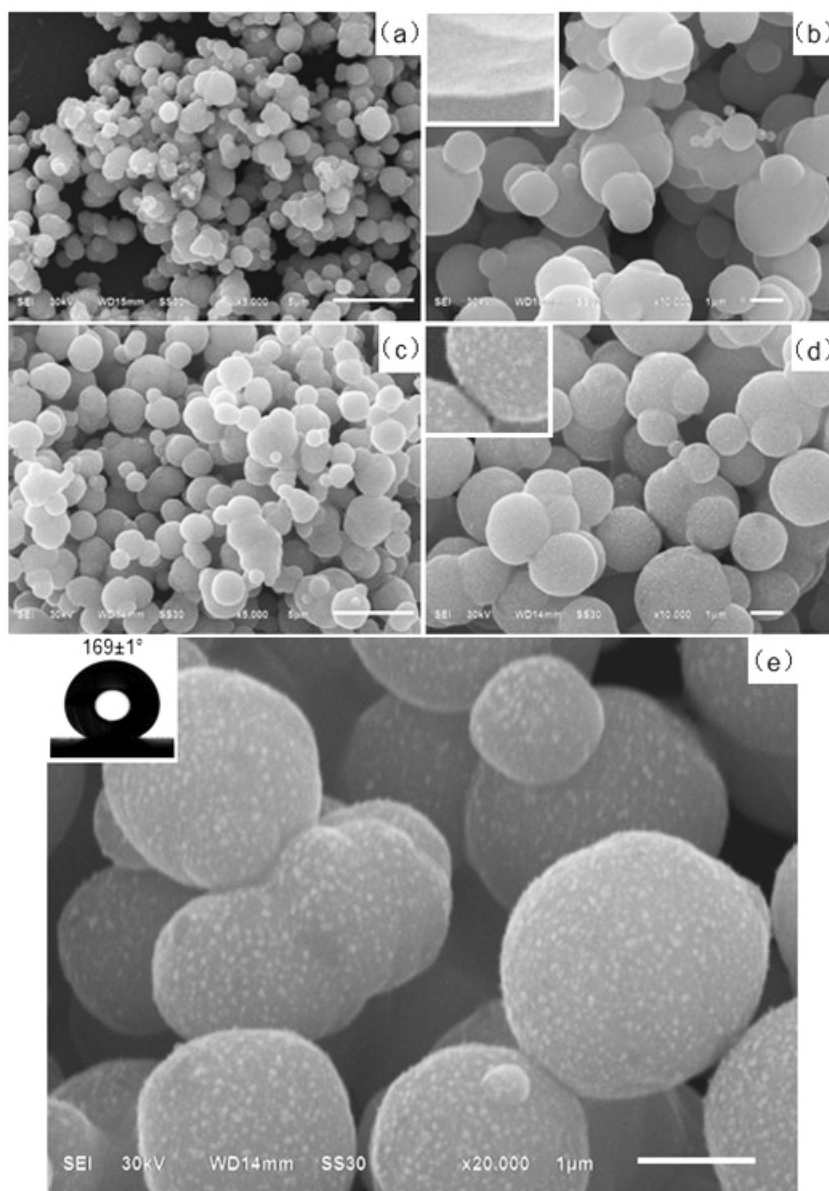
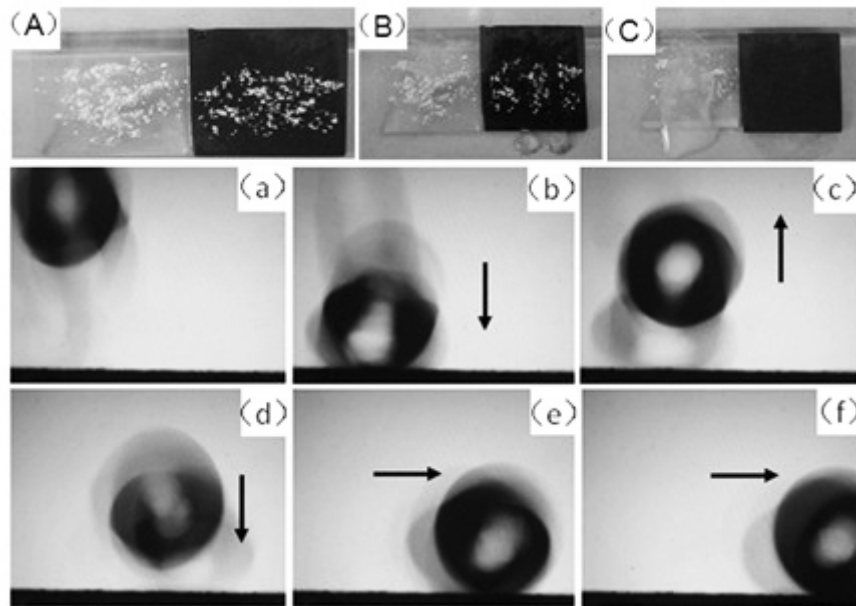


Fig. 2 - SEM images of the  $\text{Co}_3\text{O}_4$  film samples: (a),(b) sample for 60 min at low magnification and at high magnification, respectively; (c),(d) sample for 90 min at low magnification and at high magnification, respectively; (e) modified sample for 90 min

Here it is noted that the white spots are probably less than 1 nm so maybe the nanostructure term reflects more accurate the dimensions involved. The reasonable explanation for forming of nanometer particles is probably that the concentration of  $\text{Co}(\text{NO}_3)_2 \cdot 6\text{H}_2\text{O}$  becomes very low near the complete reaction. Fig. 2e shows the morphology of the  $\text{Co}_3\text{O}_4$  films (90 min) after the modification of absolute ethanol solution of stearic acids. Compared with the inset in Fig. 2d, there is almost no difference between them in structure. The phenomenon indicates that stearic acid molecule simply adhere to the  $\text{Co}_3\text{O}_4$  sphere-like surface and does not produce chemical reaction among them. It is therefore reasonable to attribute the white spots to the stearic acid molecules. Here it should be indicated that because most of the information came from SEM images in the present work, in the future further investigations should be

conducted to provide images obtained at higher magnifications and EDX analysis of the spherical particles and the white spots in order to clarify the exact morphology and composition of the film.

The static CAs and SAs (sliding angles) are measured to characterize the superhydrophobicity of the films. The inset in Fig. 2e shows the pictures of water droplets on the  $\text{Co}_3\text{O}_4$  surface coating, which indicates the coating exhibits superhydrophobic behavior with high static contact angle of approximately  $169^\circ$  after surface treatment with stearic acids. Furthermore, the coating has awfully small SA, a water droplet can hardly stand on a leveled  $\text{Co}_3\text{O}_4$  film (tilting angle of less than  $3^\circ$ , Fig. 3e and f) and would immediately roll off the surface once falling under gravitation. Such superhydrophobicity can be explained by the Cassie's theory. When a water droplet is in contact with the modified  $\text{Co}_3\text{O}_4$



**Fig. 3** - Photographs (A, B and C) of self-cleaning process. Snapshots (a-f) of the dynamic behavior of a water droplet on the superhydrophobic  $\text{Co}_3\text{O}_4$  films with slightly tilted.

films, many voids are produced in between the two due to the rough surface of  $\text{Co}_3\text{O}_4$  films micro-nanostructure. The air entrapped in the void forms a layer cushion that decreases liquid/solid contact areas between the water droplet and the film. For this reason, a water droplet on the  $\text{Co}_3\text{O}_4$  films has a quite high CA and easily slides off the films surface. The nanometer particles on the  $\text{Co}_3\text{O}_4$  sphere-like surface makes a significant contribution to the superhydrophobicity.

The first row photographs in Fig. 3 show self-cleaning performance of the superhydrophobic  $\text{Co}_3\text{O}_4$  films. From Fig. 3A, it is seen that the same amount of dust was sprinkled evenly on the common smooth surface and the superhydrophobic  $\text{Co}_3\text{O}_4$  film surface, respectively.

Naturally, the dynamic behavior of water droplets on the SHS is of more significance to the practical applications. If a free-falling water droplet vertically impacts on the superhydrophobic films with tilting angle of less than  $3^\circ$ , it will rebound a few times on the surface and rapidly escaped finally. Fig. 3(a-f) clearly show the rebounding and rolling process above. Here two possible reasons can be proposed to explain the phenomenon: the superhydrophobic films, having low surface tension because of micro-nanostructure and low surface energy of stearic acid, reduce the adhesion force to water droplets; and the air cushion intercepted in the voids of the SHS contributes to the rebounding of the droplets. In summary, the first assumption is about the low surface tension, and the second is about the air cushion effect.

The anti-icing behavior of the SHS is an important practical application in industrial and agricultural fields. Three  $9\mu\text{l}$  tap water drops were placed, respectively, on the common smooth

surface (Fig. 4a), the hydrophobic  $\text{Co}_3\text{O}_4$  surface (Fig. 4b), and the superhydrophobic  $\text{Co}_3\text{O}_4$  surface (Fig. 4c). As seen, the water drop on the common smooth surface became white and non-transparent due to freezing, whereas the other two water drops remained the same. If the delay time reached 25 min, the water drop on the hydrophobic films also changed from transparent to opaque. However, the water drop on the superhydrophobic films still kept transparent liquid ball. With the extension of time, this water drop was also changed into opaque white ball if the delay time reached 70 min. The above results indicates that the superhydrophobic  $\text{Co}_3\text{O}_4$  films showed outstanding anti-icing properties, which can delay water drop to freeze for a long time. Furthermore, for the room temperature, the water drop became liquid again and presented perfect sphericity as before icing, demonstrating that the superhydrophobic films can keep stable anti-icing properties.

In order to explain the above results, Cassie – Baxter model can be used to provide the theoretical support: **Error! Reference source not found.**, where  $\theta_r$  and  $\theta_s$  represent the water CAs on the rough and smooth surfaces, respectively, and  $f$  is the fraction of solid in contact with the liquid. The value of  $\theta_r$  and  $\theta_s$  of the glass slide is  $169^\circ$  and less than  $90^\circ$  in Fig. 4(c and a), respectively. According to the formula, more than 90% contact areas between water drop and the SHS are made up with air cushion. Because the thermal conductivity of the gas is lower than that of solid, and for the same volume of water droplets, the contact area gradually decrease with the increasing CA, thus heat loss of water droplet is relatively slow in the case of high CA. As a result, the water droplet on the superhydrophobic films can prolong the time to freeze .

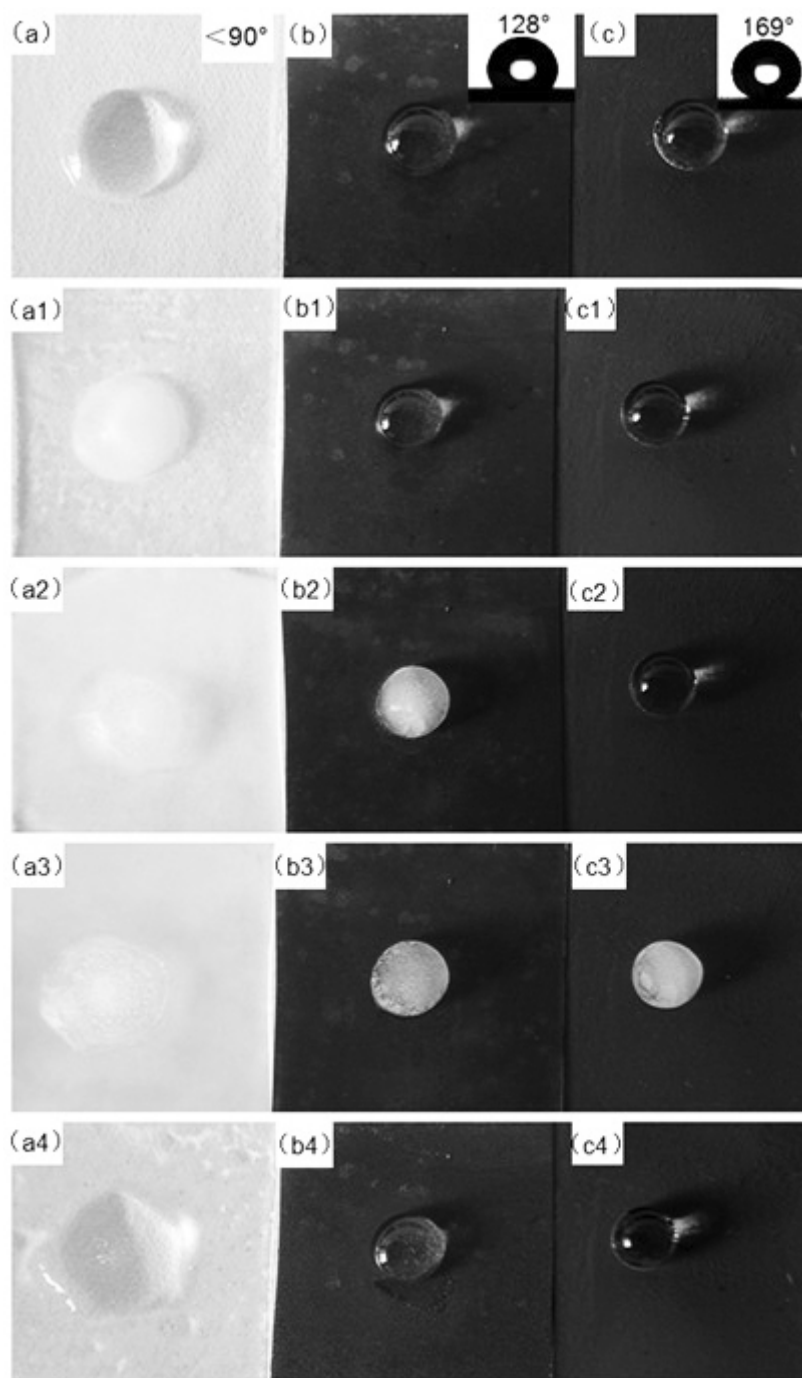


Fig. 4 - Select photographs of freeze process of water droplets on the three different surfaces at  $-5^\circ\text{C}$ . (a) common smooth surface, (b) hydrophobic  $\text{Co}_3\text{O}_4$  films surface, (c) superhydrophobic  $\text{Co}_3\text{O}_4$  films surface

#### 4. Conclusions

The superhydrophobic  $\text{Co}_3\text{O}_4$  films with a micro-nanostructure on glass slides have been successfully prepared by a simple solvothermal synthesis process at  $160^\circ\text{C}$ . The films are superhydrophobic with CA as high as approximately  $169^\circ$  and a low sliding angle of less than  $3^\circ$ . Further investigations indicate that the films possess extraordinary and stable anti-icing property. Such materials with the special function could be widely applied to various fields.

#### REFERENCES

- [1] S. Farhadi, M. Farzaneh, and S. A. Kulnich, Thermal effect on superhydrophobic performance of stearic acid modified ZnO nanotowers, *Appl. Surf. Sci.* 2011, **257**, 6264.
- [2] J. L. Laforte, M. A. Allaire, and J. Laflamme, Highly resistant icephobic coatings on aluminum alloys, *Atmos. Res.* 1998, **46**, 143.
- [3] H. Saito, K. Takai, and G. Yamauchi, Water- and ice-repellent coatings, *Surf. Coat. Int. Pt. B- C.* 1997, **80**, 168.
- [4] L. O. Andersson, C. G. Golander, and S. Persson, Controlled growth of superhydrophobic films by sol-gel method on aluminum substrate, *J. Adhes. Sci. Technol.* 1994, **8**, 117.

- [5] S. Frankenstein and A. M. Tuthill, Design of lotus-simulating surfaces: Thermodynamic analysis based on a new methodology, *J. Cold. Reg. Eng.* 2002, **16**, 83.
- [6] Y. B. Zhou, Y. Yang, W. M. Liu, Q. Ye, B. He, Y. S. Zou, P. F. Wang, X. J. Pan, W. J. Zhang, and I. Bello, Preparation of superhydrophobic Fe<sub>2</sub>O<sub>3</sub> nanorod films with the tunable water adhesion, *Appl. Phys. Lett.* 2010, **97**, 133110.
- [7] K. Liu, Z. Li, W. Wang, and L. Jiang, Bio-Inspired, Smart, Multiscale Interfacial Materials, *Appl. Phys. Lett.* 2011, **99**, 261905.
- [8] Y. H. Yeong, A. Steele, E. Loth, I. Bayer, G. D. Combarieu, and C. Lakeman, Thermodynamic analysis on superhydrophobicity based on the design of a pillar model, *Appl. Phys. Lett.* 2012, **100**, 053112.
- [9] Y. Chen, Y. Zhang, L. Shi, J. Li, Y. Xin, T. Yang, and Z. Guo, In Situ Microstructure Control of Oriented Layered Double Hydroxide Monolayer Films with Curved Hexagonal Crystals as Superhydrophobic Materials, *Appl. Phys. Lett.* 2012, **101**, 033701.
- [10] K. K. Varanasi, T. Deng, J. D. Smith, M. Hsu, and N. Bhate, Frost formation and ice adhesion on superhydrophobic surfaces, *Appl. Phys. Lett.* 2010, **97**, 234102.
- [11] L. L. Cao, A. K. Jones, V. K. Sikka, J. Z. Wu, and D. Gao, Anti-icing superhydrophobic coatings, *Langmuir*, 2009, **25**, 12444.
- [12] T. Sun, L. Feng, X. Gao, and L. Jiang, Fabrication of superhydrophobic surfaces with hierarchical structure through a solution-immersion process on copper and galvanized iron substrates, *Acc. Chem. Res.* 2005, **38**, 644.
- [13] L. Chen, M. Liu, H. Bai, P. Chen, F. Xia, D. Han, and L. Jiang, In Situ Microstructure Control of Oriented Layered Double Hydroxide Monolayer Films with Curved Hexagonal Crystals as Superhydrophobic Materials, *J. Am. Chem. Soc.* 2009, **131**, 10467.
- [14] B. J. Basu and J. Manasa, Fabrication of superhydrophobic copper by wet chemical reaction, *J. Colloid Interface Sci.* 2011, **363**, 655.

\*\*\*\*\*

## MANIFESTĂRI ȘTIINȚIFICE / SCIENTIFIC EVENTS

The 2020 edition of **Glass Performance Days South America (GPD SAME)** will be held in Sao Paulo, Brazil on the **4th of June 2020**. The event is expected to attract participants from different parts of the world. It will be held in conjunction with the **Glass South America Exhibition (3 – 6 June, 2016)** organized by Nürnberg Messe.

### Topics

#### Glass Processing

- Production Efficiency in Safety Glass Processing
  - savings in production/processing
  - new production methods
  - automation and production control systems (**internet of things**)
- How to improve glass company profitability
- Coatings Technology and Applications
- IGU & Window Technology

#### Quality and testing

- anisotropy, roller waving, end curving, optical quality
- Industry standards and regulations
  - LEED certification

#### New Technical Developments

- Industry 4.0
- New products and applications

#### Project case studies

- product and process case studies

#### Architectural design

- New creative buildings and interior design
- Architectural Challenges & Solutions
- Structural Glass Applications

#### Facades

- Glass and Sustainability in Buildings
- Smart glazing
- Facade Engineering

\*\*\*\*\*